

## University of Groningen

### Gonads or body?

van Rosmalen, Laura; van Dalum, Jayme; Hazlerigg, David G; Hut, Roelof A

*Published in:*  
The Journal of Experimental Biology

*DOI:*  
[10.1242/jeb.230987](https://doi.org/10.1242/jeb.230987)

**IMPORTANT NOTE: You are advised to consult the publisher's version (publisher's PDF) if you wish to cite from it. Please check the document version below.**

*Document Version*  
Final author's version (accepted by publisher, after peer review)

*Publication date:*  
2020

[Link to publication in University of Groningen/UMCG research database](#)

*Citation for published version (APA):*

van Rosmalen, L., van Dalum, J., Hazlerigg, D. G., & Hut, R. A. (2020). Gonads or body? Differences in gonadal and somatic photoperiodic growth response in two vole species. *The Journal of Experimental Biology*, 223. <https://doi.org/10.1242/jeb.230987>

#### Copyright

Other than for strictly personal use, it is not permitted to download or to forward/distribute the text or part of it without the consent of the author(s) and/or copyright holder(s), unless the work is under an open content license (like Creative Commons).

The publication may also be distributed here under the terms of Article 25fa of the Dutch Copyright Act, indicated by the "Taverne" license. More information can be found on the University of Groningen website: <https://www.rug.nl/library/open-access/self-archiving-pure/taverne-amendment>.

#### Take-down policy

If you believe that this document breaches copyright please contact us providing details, and we will remove access to the work immediately and investigate your claim.

*Downloaded from the University of Groningen/UMCG research database (Pure): <http://www.rug.nl/research/portal>. For technical reasons the number of authors shown on this cover page is limited to 10 maximum.*

1 Title: Gonads or body? Differences in gonadal and somatic photoperiodic growth response in  
2 two vole species.

3

4 Running title: Development of photoperiodic responses

5

6 Authors: Laura van Rosmalen<sup>1</sup>, Jayme van Dalum<sup>2</sup>, David G. Hazlerigg<sup>2</sup>, Roelof A. Hut<sup>1</sup>

7 1 Chronobiology Unit, Groningen Institute for Evolutionary Life Sciences, University of  
8 Groningen, Groningen, The Netherlands.

9 2 Department of Arctic and Marine Biology, UiT - the Arctic University of Norway,  
10 Tromsø, Norway.

11

12 Corresponding author: L.van.rosmalen@rug.nl

13

14 Keywords: Photoperiodism, seasonality, latitudinal adaptation, *Microtus*, pars tuberalis

15

16

17

18

19

20

21

22

23

24

25

26

27

28

29

30

31

32

33 Summary statement: Development of the neuroendocrine system driving photoperiodic  
34 responses in gonadal and somatic growth differ between the common and the tundra vole,  
35 indicating that they use a different breeding strategy.

36

37 List of abbreviations:

38 ARC - arcuate nucleus

39 *Dio2* - iodothyronine-deiodinase 2

40 *Dio3* - iodothyronine-deiodinase 3

41 GH - growth hormone

42 GnRH - gonadotropin-releasing hormone

43 *Kiss1* – Kisspeptin

44 KNDy - kisspeptin/neurokininB/Dynorphin

45 LP – long photoperiod

46 *Mtnr1a (Mt1)* – melatonin receptor 1a

47 *Npvf (Rfrp3)* – neuropeptide VF precursor

48 PNES – photoperiodic neuroendocrine system

49 PT – pars tuberalis

50 SCN - suprachiasmatic nucleus

51 SP – short photoperiod

52 *Tsh $\beta$*  - thyroid-stimulating-hormone- $\beta$  subunit

53 *Tshr* - thyroid-stimulating-hormone receptor

54

55

56

57

58

59

60

61

62

63

64

65

## 66 Abstract

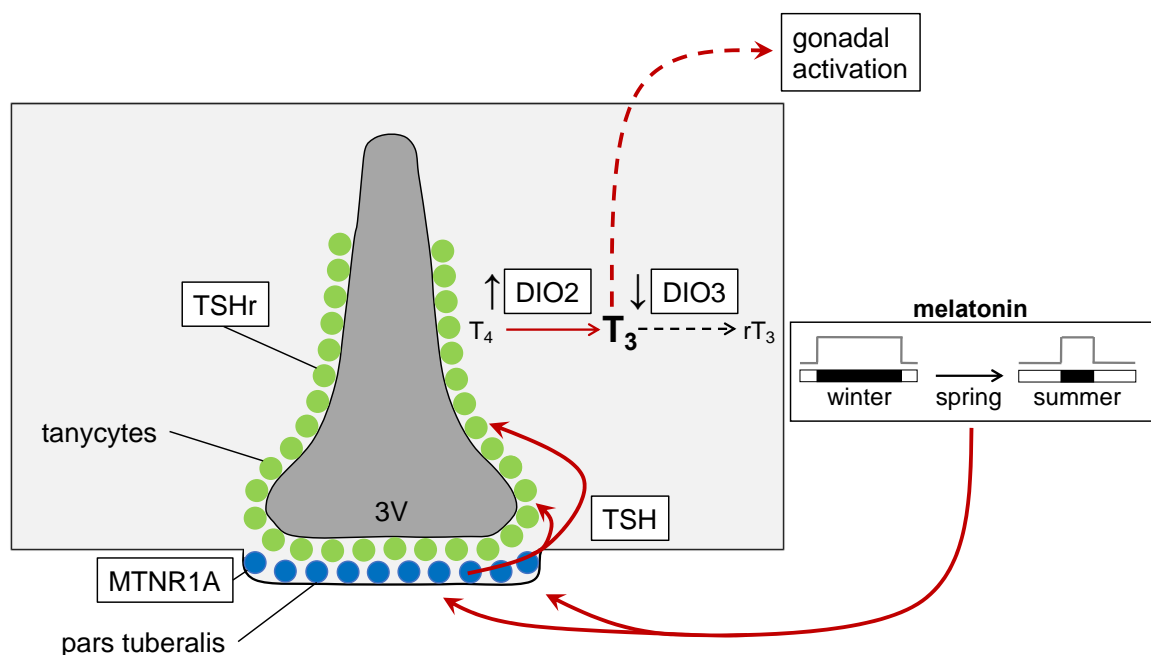
67 To optimally time reproduction, seasonal mammals use a photoperiodic neuroendocrine system  
68 (PNES) that measures photoperiod and subsequently drives reproduction. To adapt to late  
69 spring arrival at northern latitudes, a lower photoperiodic sensitivity and therefore a higher  
70 critical photoperiod for reproductive onset is necessary in northern species to arrest  
71 reproductive development until spring onset. Temperature-photoperiod relationships, and  
72 hence food availability-photoperiod relationships, are highly latitude dependent. Therefore, we  
73 predict PNES sensitivity characteristics to be latitude-dependent. Here, we investigated  
74 photoperiodic responses at different times during development in northern (tundra/root vole,  
75 *Microtus oeconomus*) and southern vole species (common vole, *Microtus arvalis*) exposed to  
76 constant short (SP) or long photoperiod (LP). Although, the tundra vole grows faster under LP,  
77 no photoperiodic effect on somatic growth is observed in the common vole. Contrastingly,  
78 gonadal growth is more sensitive to photoperiod in the common vole, suggesting that  
79 photoperiodic responses in somatic and gonadal growth can be plastic, and might be regulated  
80 through different mechanisms. In both species, thyroid-stimulating-hormone- $\beta$  subunit (*Tsh $\beta$* )  
81 and iodothyronine- deiodinase 2 (*Dio2*) expression is highly increased under LP, whereas *Tshr*  
82 and *Dio3* decreases under LP. High *Tshr* levels in voles raised under SP may lead to increased  
83 sensitivity to increasing photoperiods later in life. The higher photoperiodic induced *Tshr*  
84 response in tundra voles suggests that the northern vole species might be more sensitive to TSH  
85 when raised under SP. In conclusion, species differences in developmental programming of the  
86 PNES, which is dependent on photoperiod early in development, may form different breeding  
87 strategies evolving as part of latitudinal adaptation.

88

## 89 Introduction

90 Organisms use intrinsic annual timing mechanisms to adaptively prepare behavior, physiology,  
91 and morphology for the upcoming season. In temperate regions, decreased ambient  
92 temperature is associated with reduced food availability during winter which will impose  
93 increased energetic challenges which may, dependent on the species, prevent the possibility of  
94 successfully raising offspring. Annual variation in ambient temperature shows large  
95 fluctuations between years, with considerable day to day variations, whereas annual changes  
96 in photoperiod provide a consistent year-on-year signal for annual phase. This has led to  
97 convergent evolutionary processes in many organisms to use day length as the most reliable  
98 cue for seasonal adaptations.

99 In mammals, the photoperiodic neuroendocrine system (PNES) measures photoperiod  
 100 and subsequently drives annual rhythms in physiology and reproduction (Fig. 1) (for review  
 101 see Dardente et al., 2018; Hut, 2011; Nakane and Yoshimura, 2019). The neuroanatomy of this  
 102 mechanism has been mapped in detail and genes and promoter elements that play a crucial role  
 103 in this response pathway have been identified in several mammalian species (Dardente et al.,  
 104 2010; Hanon et al., 2008; Hut, 2011; Masumoto et al., 2010; Nakao et al., 2008; Ono et al.,  
 105 2008; Sáenz De Miera et al., 2014; Wood et al., 2015), including the common vole (Król et al.,  
 106 2012).



107  
 108 **Figure 1. The photoperiodic neuroendocrine system (PNES) of a long-day breeding mammal.** Light is  
 109 perceived by specialized mammalian non-visual retinal photoreceptors that signal to the suprachiasmatic nucleus  
 110 (SCN). The SCN acts via the paraventricular nucleus (PVN) on the pineal gland, such that the duration of  
 111 melatonin production during darkness changes over the year to represent the inverse of day length. Melatonin  
 112 binds to its receptor (MTNR1A/ MT1) in the pars tuberalis (PT) of the anterior lobe of the pituitary gland (Gall  
 113 et al., 2002; Gall et al., 2005; Klosen et al., 2019; Williams and Morgan, 1988). Under long days, pineal melatonin  
 114 is released for a short duration and thyroid stimulating hormone  $\beta$  subunit (Tsh $\beta$ ) is increased in the pars tuberalis,  
 115 forming an active dimer (TSH) with chorionic gonadotropin  $\alpha$ -subunit ( $\alpha$ -GSU) (Magner, 1990). PT-derived TSH  
 116 acts locally through TSH receptors (TSHr) found in the tanycytes in the neighbouring mediobasal hypothalamus  
 117 (MBH). The tanycytes produce increased iodothyronine deiodinase 2 (DIO2) and decreased DIO3 levels (Guerra  
 118 et al., 2010; Hanon et al., 2008; Nakao et al., 2008), which leads to higher levels of the active form of thyroid  
 119 hormone (T<sub>3</sub>) and lower levels of inactive forms of thyroid hormone (T<sub>4</sub> and rT<sub>3</sub>) (Lechan and Fekete, 2005). In  
 120 small mammals, it is likely that T<sub>3</sub> acts 'indirectly', through KNDy (kisspeptin/neurokininB/Dynorphin) neurons  
 121 of the arcuate nucleus (ARC) (for review see Simonneaux, 2020) in turn controlling the activity of gonadotropin-

122 releasing hormone (GnRH) neurons. GnRH neurons project to the pituitary to induce gonadotropin release, which  
123 stimulates gonadal growth. Arrow connectors indicate stimulatory connections.

124

125 Voles are small grass-eating rodents with a short gestation time (i.e. 21 days). They can  
126 have several litters a year, while their offspring can reach sexual maturity within 40 days during  
127 spring and summer. Overwintering voles may however delay reproductive activity by as much  
128 as 7 months (Wang et al., 2019). In small rodents, photoperiods experienced early in  
129 development determines growth rate and reproductive development. Photoperiodic reactions  
130 to intermediate day lengths depend on prior photoperiodic exposure (Hoffmann, 1973; Horton,  
131 1984a; Horton, 1984b; Horton, 1985; Horton and Stetson, 1992; Prendergast et al., 2000; Sáenz  
132 de Miera et al., 2017; Stetson et al., 1986; Yellon and Goldman, 1984). By using information  
133 about day length early in life, young animals will be prepared for the upcoming season.  
134 Presumably, crucial photoperiod-dependent steps in PNES development take place in young  
135 animals to secure an appropriate seasonal response later in life (Dalum et al., 2020; Sáenz de  
136 Miera et al., 2017; Sáenz de Miera et al., 2020; Sáenz De Miera, 2019). In Siberian hamsters,  
137 photoperiodic programming takes place downstream of melatonin secretion at the level of *Tshr*,  
138 with expression increased in animals born under SP, associated with subsequent increases in  
139 TSH sensitivity (Sáenz de Miera et al., 2017).

140 Primary production in the food web of terrestrial ecosystems is temperature-dependent  
141 (Robson, 1967; Peacock, 1976; Malyshev *et al.*, 2014). Small herbivores may therefore show  
142 reproductive development either as a direct response to temperature increases (opportunistic  
143 response), or as a response to photoperiod which forms an annual proxy for seasonal  
144 temperature changes (photoperiodic response), or a combination of the two (Caro et al., 2013).  
145 *Microtus* species adjust their photoperiodic response such that reproduction in spring starts  
146 when primary food production starts (Baker, 1938).

147 Photoperiodically induced reproduction should start at longer photoperiods at more  
148 northern populations, since a specific ambient spring temperature at higher latitudes coincides  
149 with longer photoperiods compared to lower latitudes (Hut et al., 2013). To adapt to late spring  
150 arrival at northern latitudes, a lower sensitivity to photoperiod, and therefore, a longer critical  
151 photoperiod is expected to be necessary in northern species. This is crucial to arrest  
152 reproductive development until arrival of spring. Moreover, (epi)genetic adaptation to local  
153 annual environmental changes may create latitudinal differences in photoperiodic responses  
154 and annual timing mechanisms.

155 *Microtus* is a genus of voles found in the northern hemisphere, ranging from close to  
156 the equator to arctic regions, which makes it an excellent genus to study latitudinal adaptation  
157 of photoperiodic responses (for review see Hut et al., 2013). In order to understand the  
158 development of the PNES for vole species with different paleogeographic origins, we  
159 investigated photoperiodic responses at different time points during development by exposing  
160 northern- (tundra/root vole, *Microtus oeconomus* (Pallas, 1776)) and southern vole species  
161 (common vole, *Microtus arvalis* (Pallas, 1778)) to constant short- or long photoperiods in the  
162 laboratory. Animals from our two vole lab populations originate from the same latitude in the  
163 Netherlands (53°N) where both populations overlap. This is for the common vole the center  
164 (mid-latitude) of its distribution range (38-62°N), while our lab tundra voles originate from a  
165 postglacial relict population at the southern boundary of its European geographical range (48-  
166 72°N). Assuming that the latitudinal distribution range is limited by seasonal adaptation, it is  
167 expected that latitudinal adaptation is optimal at the center of the distribution and suboptimal  
168 towards the northern and southern boundaries. Although this assumption remains to be  
169 confirmed at the genetic and physiological level, it does lead to the expectation that the PNES  
170 of the common vole is better adapted to the local annual environmental changes of the  
171 Netherlands (53°N, distribution center) than that of the tundra vole which is at its southern  
172 distribution boundary. Because lower latitudes have higher spring temperatures at a specific  
173 photoperiod (Hut et al., 2013), we hypothesize that gonadal activation through PNES signaling  
174 occurs under shorter photoperiods in common voles than in tundra voles.

175

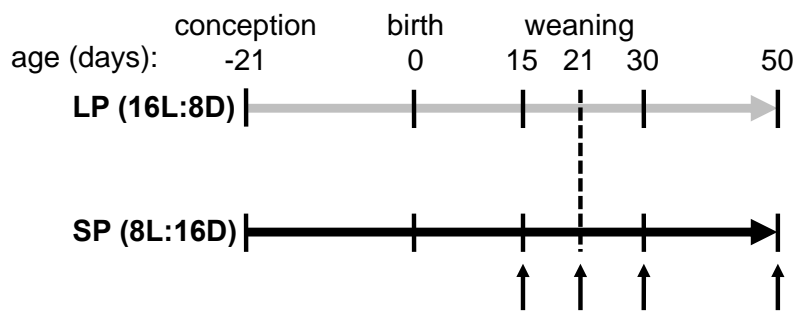
## 176 Materials and methods

### 177 *Animals and experimental procedures*

178 All experimental procedures were carried out according to the guidelines of the animal welfare  
179 body (IvD) of the University of Groningen, and all experiments were approved by the Centrale  
180 Commissie Dierproeven) of the Netherlands (CCD, license number: AVD1050020171566).  
181 The Groningen common vole breeding colony started with voles (*M. arvalis*) obtained from the  
182 Lauwersmeer area (Netherlands, 53° 24' N, 6° 16' E) (Gerkema et al., 1993), and was  
183 occasionally supplemented with wild caught voles from the same region to prevent the lab  
184 population from inbreeding. The Groningen tundra vole colony started with voles (*M.*  
185 *oeconomus*) obtained from four different regions in the Netherlands (described in Van de  
186 Zande et al., 2000). Both breeding colonies were maintained at the University of Groningen as  
187 outbred colonies and provided the voles for this study. All breeding pairs were kept in climate  
188 controlled rooms, at an ambient temperature of 21 ±1°C and 55 ±5% relative humidity and

189 housed in transparent plastic cages (15 x 40 x 24 cm) provided with sawdust, dried hay, an  
190 opaque pvc tube and *ad libitum* water and food (standard rodent chow, #141005; Altromin  
191 International, Lage, Germany). Over the last four years, our captive lab populations are housed  
192 under LP conditions (16h light: 8h dark) and switched to SP (8h light: 16h dark) for ~2 months  
193 at least twice a year.

194 The voles used in the experiments (61 males, 56 females) were both gestated and born  
195 under either a long photoperiod (LP, 16h light: 8h dark) or a short photoperiod (SP, 8h light:  
196 16h dark). In the center of the distribution range of *M. arvalis*, 16L:8D in spring occurs on 17  
197 May, and 8L:16D occurs on 13 January. In the center of the distribution range of *M.*  
198 *oeconomus*, 16L:8D in spring occurs on 1 May, and 8L:16D occurs on 1 February. Maximum  
199 and minimum photoperiods experienced by *M. arvalis* and *M. oeconomus* at the center of its  
200 distributional range are 17L:7D, 7.5L:16.5D, 19L:5D, 6L:18D respectively. Pups were weaned  
201 and transferred to individual cages (15 x 40 x 24 cm) when 21 days old but remained exposed  
202 to the same photoperiod as during both gestation and birth. All voles were weighed at post-  
203 natal day 7, 15, 21, 30, 42 and 50 (Fig. 2).



204  
205 **Figure 2. Experimental design.** Animals were constantly exposed to either LP or SP from gestation onwards.  
206 Arrows indicate sampling points for tissue collection. Age in days is depicted above the timeline. Vertical dashed  
207 line represents time of weaning (21 days old).  
208

### 209 *Tissue collections*

210 In order to follow development, animals were sacrificed by decapitation  $17 \pm 1$  hours after lights  
211 off (*Tsh $\beta$*  expression peaking in pars tuberalis (Masumoto et al., 2010)), at an age of 15, 21, 30  
212 and 50 days old. Brains were removed with great care to include the stalk of the pituitary  
213 containing the pars tuberalis. The hypothalamus with the pars tuberalis were dissected as  
214 described in Prendergast et al., 2013: the optic chiasm at the anterior border, the mammillary  
215 bodies at the posterior border, and laterally at the hypothalamic sulci. The remaining  
216 hypothalamic block was cut dorsally 3-4 mm from the ventral surface. The extracted  
217 hypothalamic tissue was flash frozen in liquid N<sub>2</sub> and stored at -80°C until RNA extraction.



218 Reproductive organs were dissected and cleaned of fat, and wet masses of paired testis, paired  
219 ovary and uterus were measured ( $\pm 0.0001$  g).

220

#### 221 *RNA extraction, Reverse Transcription and Real-time quantitative PCR*

222 Total RNA was isolated from the dissected part of the hypothalamus using TRIzol reagent  
223 according to the manufacturer's protocol (Invitrogen™, Carlsbad, California, United States).  
224 In short, frozen pieces of tissue (~0.02 g) were homogenized in 0.5 ml TRIzol reagent in a  
225 TissueLyser II (Qiagen, Hilden, Germany) (2 x 2 minutes at 30 Hz) using tubes containing a  
226 5mm RNase free stainless-steel bead. Subsequently 0.1 ml chloroform was added for phase  
227 separation. Following RNA precipitation by 0.25 ml of 100% isopropanol, the obtained pellet  
228 was washed with 0.5 ml of 75% ETOH. Depending on the size, RNA pellets were diluted in  
229 an adequate volume of RNase-free H<sub>2</sub>O (range 20-50  $\mu$ L) and quantified on a Nanodrop 2000  
230 (Thermoscientific™, Waltham, Massachusetts, United States). RNA concentrations were  
231 between 109-3421 ng/ $\mu$ L and ratio of the absorbance at 260/280 nm was between 1.62-2.04.  
232 After DNA removal by DNase I treatment (Invitrogen™, Carlsbad, California, United  
233 States), equal quantity of RNA from each sample was used for cDNA synthesis by using  
234 RevertAid H minus first strand cDNA synthesis reagents (Thermoscientific™, Waltham,  
235 Massachusetts, United States). 40  $\mu$ L Reverse Transcription (RT) reactions were prepared  
236 using 2  $\mu$ g RNA, 100  $\mu$ M Oligo(dT)<sub>18</sub>, 5x Reaction buffer, 20 U/ $\mu$ L RiboLock RNase  
237 Inhibitor, 10 mM dNTP Mix, RevertAid H Minus Reverse Transcriptase (200 U/ $\mu$ L).  
238 Concentrations used for RT reactions can be found in the supplementary information (table  
239 S1). RNA was reversed transcribed by using a thermal cycler (S1000™, Bio-Rad, Hercules,  
240 California, United States). Incubation conditions used for RT were: 45°C for 60 minutes  
241 followed by 70°C for 5 minutes. Transcript levels were quantified by Real-Time qPCR using  
242 SYBR Green (KAPA SYBR FAST qPCR Master Mix, Kapa Biosystems). 20  $\mu$ L (2  $\mu$ L  
243 cDNA + 18  $\mu$ L Mastermix) reactions were carried out in duplo for each sample by using 96-  
244 well plates in a Fast Real-Time PCR System (CFX96, Bio-Rad, Hercules, California, United  
245 States). Primers for genes of interest were designed using Primer-BLAST (NCBI) and  
246 optimized annealing temperature (T<sub>m</sub>) and primer concentration. All primers used in this  
247 study were designed based on the annotated *Microtus ochrogaster* genome (NCBI:txid79684,  
248 GCA\_000317375.1), and subsequently checked for gene specificity in the genomes of the  
249 common vole (*Microtus arvalis*) and the tundra vole (*Microtus oeconomus*), which were  
250 published by us on NCBI (NCBI:txid47230, GCA\_007455615.1 and NCBI:txid64717,  
251 GCA\_007455595.1) (tableS2). Thermal cycling conditions used can be found in the

252 supplementary information (table S3). Relative mRNA expression levels were calculated  
253 based on the  $\Delta\Delta\text{CT}$  method using *Gapdh* as the reference (housekeeping) gene (Pfaffl 2001).

254

#### 255 *Statistical analysis*

256 Sample size ( $n = 4$ ) was determined by a power calculation ( $\alpha = 0.05$ , power = 0.80) based on  
257 the effect size ( $d = 2.53$ ) of an earlier study, in which gonadal weight was assessed in female  
258 voles under three different photoperiods (Król et al., 2012). Effects of age, photoperiod and  
259 species on body mass, reproductive organs and gene expression levels were determined using  
260 a type I two-way ANOVA. Tukey HSD post-hoc pairwise comparisons were used to compare  
261 groups at specific ages. Statistical significance was determined at  $p < 0.05$ . Statistical results  
262 can be found in the supplementary information (table S4). All statistical analyses were  
263 performed using RStudio (version 1.2.1335) (R Core Team, 2013), and figures were generated  
264 using the ggplot2 package (Wickham, 2016).

265

## 266 Results

### 267 *Body mass responses for males and females*

268 Photoperiod during gestation did not affect birth weight in either species (Fig. 3A,B). Both  
269 tundra vole males and females grow faster under LP compared to SP conditions (males,  $F_{1,303}$   
270 = 15.0,  $p < 0.001$ ; females,  $F_{1,307} = 10.2$ ,  $p < 0.01$ ) (Fig. 3A,B). However, no effect of  
271 photoperiod on body mass over time was observed in common vole males or females (males,  
272  $F_{1,243} = 2.1$ , ns; females,  $F_{1,234} = 0.6$ , ns) (Fig. 3A,B).

273

### 274 *Gonadal responses for males*

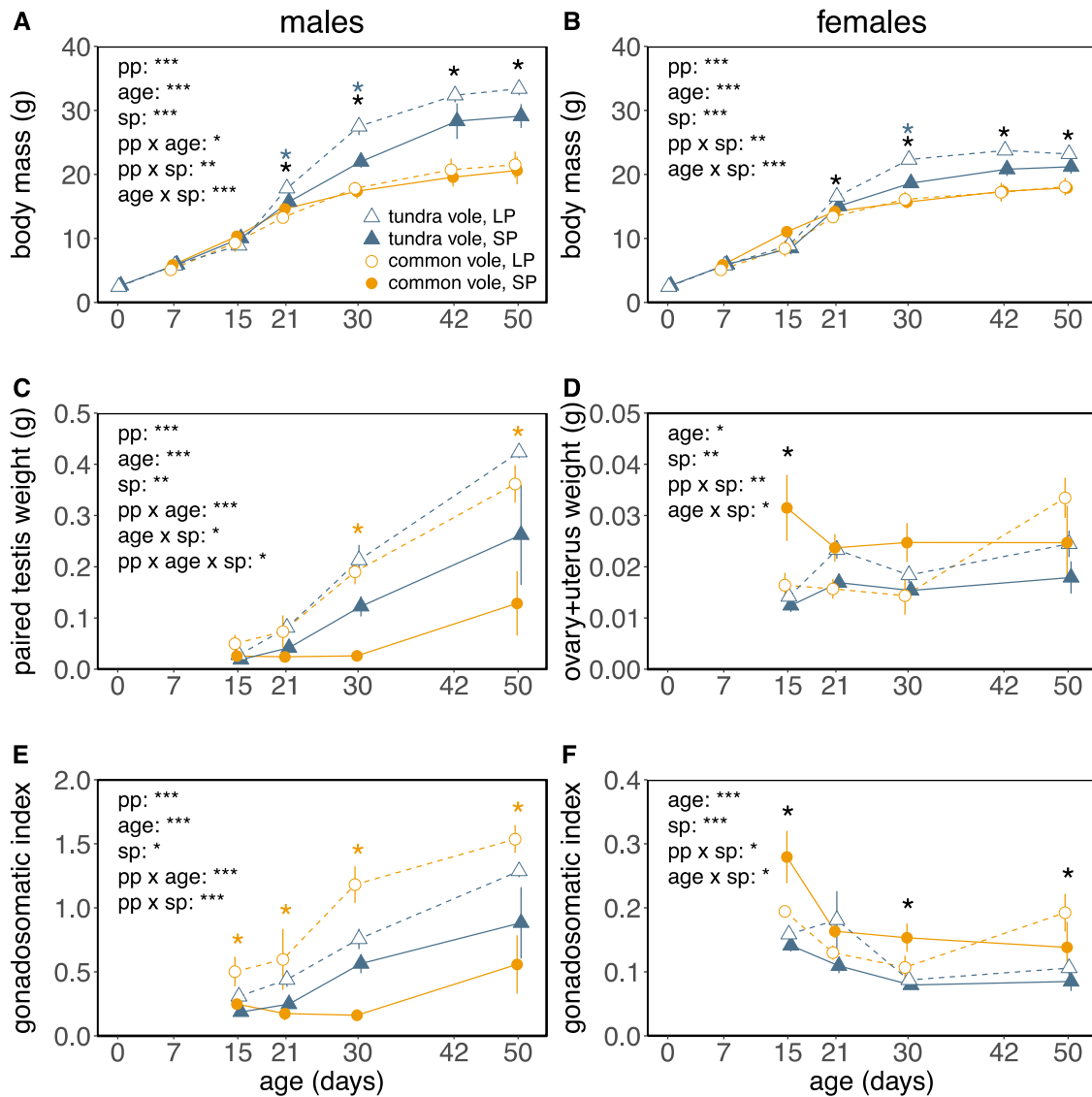
275 Common vole males show faster testis growth under LP compared to SP (testis,  $F_{1,33} = 17.01$ ,  
276  $p < 0.001$ ; GSI,  $F_{1,33} = 32.2$ ,  $p < 0.001$ ) (Fig. 3C,E). This photoperiodic effect on testis  
277 development is less pronounced in tundra voles (testis,  $F_{1,35} = 8.3$ ,  $p < 0.01$ ; GSI,  $F_{1,35} = 9.3$ ,  $p$   
278  $< 0.01$ ) (Fig. 3C,E).

279

### 280 *Gonadal responses for females*

281 Common vole female gonadal weight (i.e. paired ovary + uterus) is slightly higher in the  
282 beginning of development (until 30 days old) under SP compared to LP conditions ( $F_{1,17} =$   
283 10.4,  $p < 0.01$ ) (Fig. 3D), while the opposite effect was observed in tundra voles ( $F_{1,36} = 9.0$ ,  $p$   
284  $< 0.01$ ) (Fig. 3D). For both species, these photoperiodic effects disappeared when gonadal mass  
285 was corrected for body mass (common vole,  $F_{1,17} = 2.5$ , ns; tundra vole,  $F_{1,36} = 2.3$ , ns) (Fig.

286 3F). Interestingly, gonadal weight is significantly increasing in 30-50 days old LP common  
 287 vole females ( $F_{1,5} = 7.7, p < 0.05$ ) (Fig. 3D), but not in tundra vole ( $F_{1,11} = 2.2, ns$ ) or under SP  
 288 conditions (common vole,  $F_{1,7} = 0, ns$ ; tundra,  $F_{1,7} = 1.0, ns$ ).  
 289



290  
 291 **Figure 3. Effects of constant photoperiod on growth and gonadal development.** Graphs show body mass  
 292 growth curves for (A) males and (B) females, (C) paired testis weight, (D) paired ovary + uterus weight,  
 293 (E, F) gonadal development relative to body mass (gonadosomatic index) for common voles (orange circles) and  
 294 tundra voles (blue triangles), continuously exposed to either LP (open symbols, dashed lines) or SP (closed  
 295 symbols, solid lines). Lines connect averages representing non-repeated measures. Data are mean±s.e.m. Male  
 296 tundra vole LP: n=22, male tundra vole SP: n=15, male common vole LP n=19, male common vole SP n=16.  
 297 female tundra vole LP: n=21, female tundra vole SP: n=17, female common vole LP n=12, female common vole  
 298 SP n=16. Significant effects (type I two-way ANOVA's, post-hoc Tukey) of photoperiod at specific ages are  
 299 indicated for tundra voles (blue asterisks) and common voles (orange asterisks). Significant effects of species are  
 300 indicated by black asterisks. Significant effects of: photoperiod (pp), age (age), species (sp) and interactions are

301 shown in each graph, \*  $p < 0.05$ , \*\*  $p < 0.01$ , \*\*\*  $p < 0.001$ . Statistic results for ANOVA's (photoperiod, age and  
302 species) can be found in table S4.

303

#### 304 *Photoperiod induced changes in hypothalamic gene expression*

305 Melatonin binds to its receptors in the pars tuberalis where it inhibits *Tsh $\beta$*  expression. In males  
306 of both species, *Mtnr1a* (*Mt1*, melatonin receptor) expression in the hypothalamic block with  
307 preserved pars tuberalis was highly expressed, but unaffected by photoperiod or age  
308 (photoperiod,  $F_{1,43} = 0.08$ , ns; age,  $F_{3,42} = 0.94$ , ns) (Fig. 4A). In females, *Mtnr1a* expression  
309 increases approximately 2-fold with age in both species ( $F_{3,40} = 9.04$ ,  $p < 0.001$ ) (Fig. 4B), but  
310 no effects of photoperiod were observed ( $F_{1,40} = 1.59$ , ns).

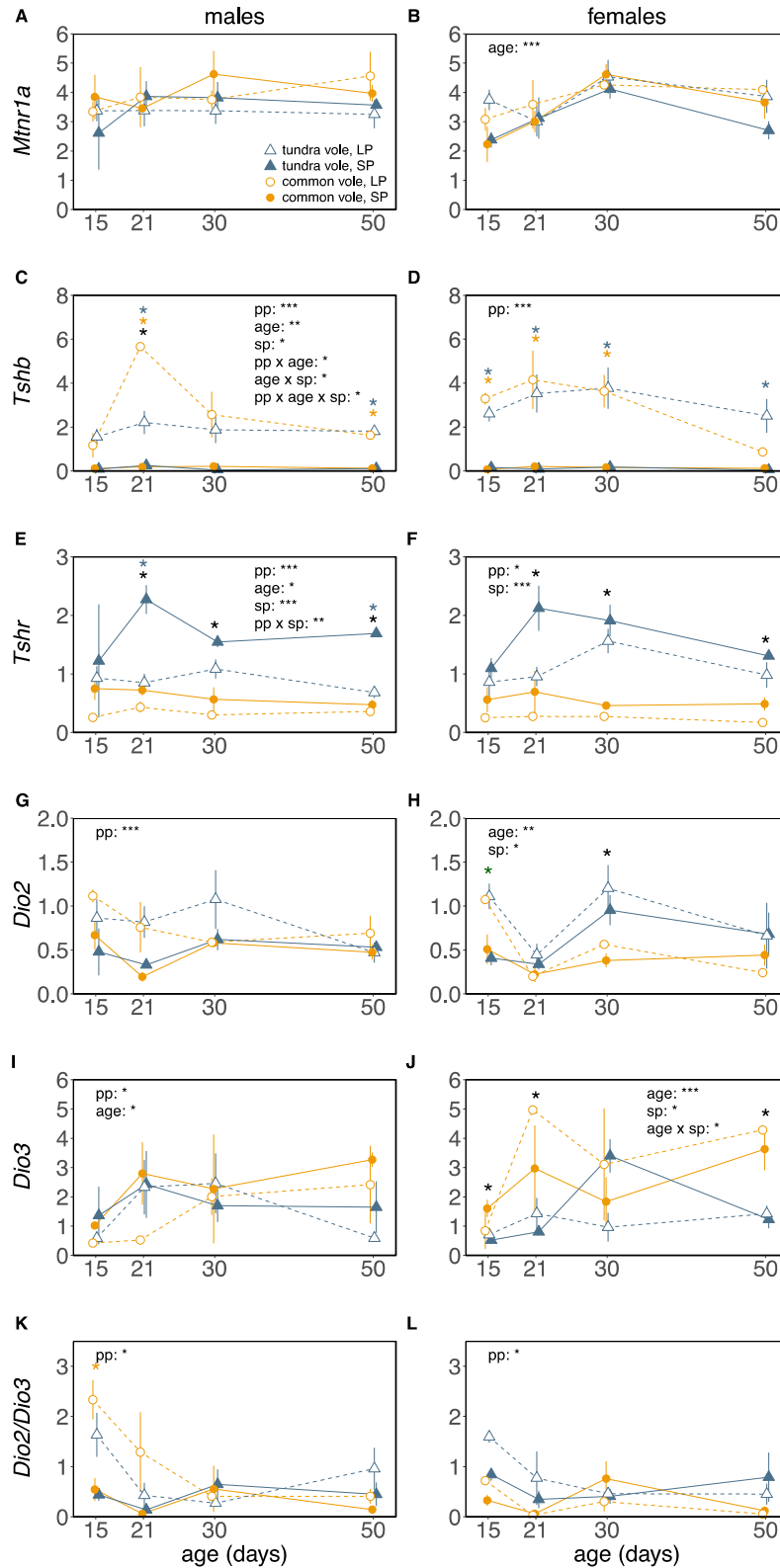
311 In males and females of both species, *Tsh $\beta$*  expression is dramatically elevated under  
312 LP throughout development (tundra vole males,  $F_{1,27} = 49.3$ ,  $p < 0.001$ ; common vole males,  
313  $F_{1,27} = 21.3$ ,  $p < 0.001$ ; tundra vole females,  $F_{1,30} = 63.7$ ,  $p < 0.001$ ; common vole females,  $F_{1,22}$   
314  $= 60.9$ ,  $p < 0.001$ ) (Fig. 4C,D). Furthermore, a clear peak in *Tsh $\beta$*  expression is observed in 21-  
315 day old LP common vole males, while such a peak is lacking in tundra vole males. On the other  
316 hand, *Tsh $\beta$*  expression in tundra vole males remains similar over the course of development  
317 under LP conditions. In females, photoperiodic responses on *Tsh $\beta$*  expression did not differ  
318 between species ( $F_{1,40} = 0.02$ , ns).

319 TSH $\beta$  binds to its receptor (TSHr) in the tanycytes around the third ventricle. In tundra  
320 vole males and females, *Tshr* expression is higher under SP compared to LP (males,  $F_{1,27} =$   
321  $23.7$ ,  $p < 0.001$ ; females,  $F_{1,30} = 6.2$ ,  $p < 0.05$ ) (Fig. 4E,F), while photoperiodic induced changes  
322 in *Tshr* expression are smaller in common vole males and females (males,  $F_{1,27} = 23.7$ ,  $p <$   
323  $0.01$ ; females,  $F_{1,22} = 4.3$ ,  $p < 0.05$ ) (Fig. 4E,F). Photoperiodic responses on *Tshr* expression  
324 are significantly larger in tundra vole males compared to common vole males ( $F_{1,42} = 8.17$ ,  $p$   
325  $< 0.01$ ) (Fig. 4E).

326 In males of both species, the largest photoperiodic effect on *Dio2*, which is **increased**  
327 by TSH $\beta$ , is found at weaning (day 21), with higher levels under LP compared to SP ( $F_{1,42} =$   
328  $14.7$ ,  $p < 0.001$ ) (Fig. 4G). Interestingly, *Dio3* is lower in these animals ( $F_{1,42} = 4.8$ ,  $p < 0.05$ )  
329 (Fig. 4I), leading to a high *Dio2/Dio3* ratio under LP in the beginning of development ( $F_{1,42} =$   
330  $8.5$ ,  $p < 0.01$ ) (Fig. 4K). We find a similar pattern in females, with higher *Dio2* under LP  
331 compared to SP at the beginning of development (i.e. day 15) ( $F_{3,10} = 8.9$ ,  $p < 0.01$ ) (Fig. 4H).

332 In males of both species, no effects of photoperiod on Eyes Absent 3 (*Eya3*,  
333 transcription factor for the *Tsh $\beta$*  promoter) ( $F_{1,42} = 1.72$ , ns), Kisspeptin (*Kiss1*, hypothalamic  
334 gene involved in reproduction) ( $F_{1,42} = 2.96$ , ns) and Neuropeptide VF precursor (*Npvf*, *Rfrp3*,

335 hypothalamic gene involved in seasonal growth and reproduction) ( $F_{1,42} = 0.61$ , ns) expression  
 336 were found (Fig. S1A,C,E). In females, both *Kiss1* ( $F_{3,40} = 4.82$ ,  $p < 0.01$ ) and *Npvf* is higher  
 337 under LP dependent on age ( $F_{3,40} = 3.51$ ,  $p < 0.05$ ) (Fig. S1D,F), but there were no effects of  
 338 photoperiod on *Eya3* ( $F_{1,40} = 0.30$ , ns (Fig. S1B).



340 **Figure 4. Effects of constant photoperiod on gene expression levels in the developing hypothalamus.** Graphs  
 341 show relative gene expression levels of (A, B) *Mtnr1a*, (C, D) *Tshb*, (E, F) *Tshr*, (G, H) *Dio2*, (I, J) *Dio3* and (K,  
 342 L) *Dio2/Dio3* expression in the hypothalamus of developing common vole (orange circles) and tundra vole (blue  
 343 triangles) males and females respectively, under LP (open symbols, dashed lines) or SP (closed symbols, solid  
 344 lines). Lines connect averages representing non-repeated measures. Data are mean $\pm$ s.e.m. Male tundra vole LP:  
 345 n=16, male tundra vole SP: n=13, male common vole LP n=14, male common vole SP n=15. female tundra vole  
 346 LP: n=16, female tundra vole SP: n=16, female common vole LP n=8, female common vole SP n=16. Significant  
 347 effects (type I two-way ANOVA's, post-hoc Tukey) of photoperiod at specific ages are indicate for tundra voles  
 348 (blue asterisks) and common voles (orange asterisks). Significant effects of species are indicated by black  
 349 asterisks. Significant effects of: photoperiod (pp), age (age), species (sp) and interactions are shown in each graph,  
 350 \* $p < 0.05$ , \*\* $p < 0.01$ , \*\*\* $p < 0.001$ . Statistic results for ANOVA's (photoperiod, age and species) can be found in  
 351 table S4.

352

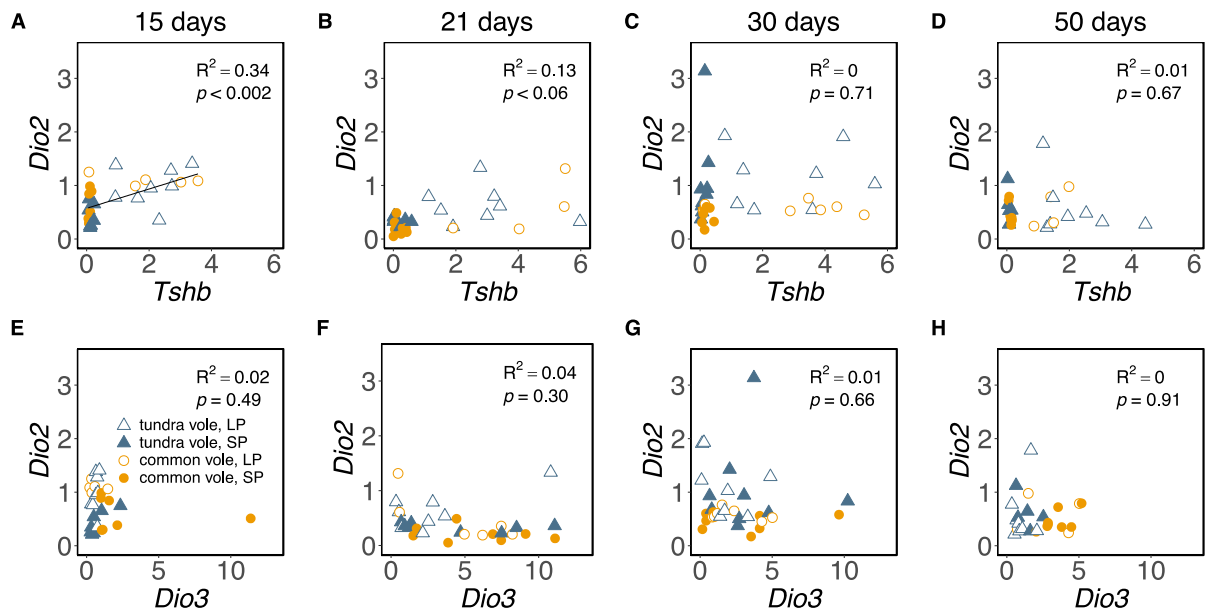
353 A positive correlation between the levels of *Tshb* and *Dio2* expression was found only  
 354 at the beginning of development (15 days,  $F_{1,25} = 12.6$ ,  $p < 0.01$ ; 21 days,  $F_{1,28} = 4.0$ ,  $p < 0.1$ ;  
 355 30 days,  $F_{1,30} = 0.1$ , ns; 50 days,  $F_{1,23} = 0.1$ , ns) (Fig. 5A-D). Moreover, no significant  
 356 relationship between *Dio2* and *Dio3* expression was found (Fig. 5E-H).

357

358

359

360



361

362

363

364

365 **Figure 5. Relationship between hypothalamic *Dio2*, *Dio3* and *Tsh $\beta$*  expression in voles at different age.**  
366 Scatterplot of *Tsh $\beta$*  versus *Dio2* gene expression at (A) 15, (B) 21, (C) 30 and (D) 50 days old. Scatterplot of *Dio3*  
367 versus *Dio2* gene expression at (E) 15, (F) 21, (G) 30 and (H) 50 days old. Open symbols indicate LP animals,  
368 closed symbols indicate SP animals. Blue triangles represent tundra voles, orange circles represent common voles.  
369 One outlier in *Dio2* expression was detected by an outlier analysis, however removing the outlier did not change  
370 the fitted linear models.

371

## 372 Discussion

373 This study demonstrates different effects of constant photoperiod on the PNES in two different  
374 vole species: the common vole and the tundra vole. Overall, somatic growth is  
375 photoperiodically sensitive in the tundra vole while gonadal growth is photoperiodically  
376 sensitive in the common vole. Hypothalamic *Tsh $\beta$* , *Tshr*, *Dio2* and *Dio3* expression is highly  
377 affected by photoperiod and age, and some species differences were observed in the magnitude  
378 of these effects. Although the differences found between both vole species may provide  
379 interesting information on variation in annual timing, the data should be interpreted with  
380 caution because we cannot exclude relaxation of natural selection in our laboratory colonies.

381

### 382 *Photoperiod induced changes in somatic growth and gonadal development*

383 These data demonstrate that photoperiod early in life affects pup growth in tundra vole (Fig.  
384 3A), and reproductive development in common vole males (Fig. 3C,E). In females, a similar  
385 photoperiodic effect on somatic growth is observed as in males. Tundra vole females grow  
386 faster under LP compared to SP, while there is no difference in growth rate between LP and  
387 SP in the common vole (Fig. 3B). In the tundra vole, somatic growth is plastic, whereas, in the  
388 common vole, gonadal growth is plastic. Garden dormouse (*Eliomys quercinus*) born late in  
389 the season grow and fatten twice as fast as early born animals (Stumpfel et al., 2017), in order  
390 to partly compensate for the limited time before winter onset. This overwintering strategy  
391 might be favorable for animals with a short breeding season (i.e. at high latitude), and may also  
392 be used in tundra voles since they gain weight faster when raised under LP (i.e. late in the  
393 season) compared to SP (i.e. early in the season). Southern arvicoline species have longer  
394 breeding seasons (Tkadlec, 2000), and therefore have more time left to compensate body mass  
395 when born late in the season. Therefore, somatic growth rate may depend to a lesser extent on  
396 the timing of birth in southern species as observed in common voles raised under SP or LP.

397 Common vole female gonadal weight is slightly higher under SP compared to LP at the  
398 beginning of development (Fig. 3D,F). In contrast, in Siberian hamsters, uterus weight is

399 increased after 3 weeks of constant LP exposure, which continued throughout development  
400 (Ebling, 1994; Phalen et al., 2009). In common voles, female gonadal weight is increasing from  
401 day 30 to day 50 in LP animals, whereas gonadal weight in SP females remains the same (Fig.  
402 3D,F). Also, tundra vole female gonadal weight is not increased in this period of development  
403 under both LP and SP conditions. Puberty onset, based on gonadal weight, in common voles is  
404 later in time compared to Siberian hamsters (Phalen et al., 2009), while earlier in time  
405 compared to tundra voles. Therefore, LP common voles increase gonadal weight earlier in  
406 development (i.e. > 30 days old) compared to LP tundra voles (i.e. > 50 days old), in order to  
407 increase reproductive activity and prepare for pregnancy. An alternative hypothesis is that the  
408 tundra vole may sense 16:8 not as too short for spring stimulation of reproduction, but rather  
409 as too long to switch off reproduction in autumn. These results suggest that tundra vole females  
410 have a different reproductive onset compared to common vole females under constant  
411 photoperiods. However, based on our data we cannot conclude whether the timing of the  
412 breeding season is different between those species, since we did not use naturally changing  
413 photoperiods to simulate different seasons. This can be tested by exposing voles to a broader  
414 range of different photoperiod regimes, mimicking spring and autumn photoperiod conditions  
415 in the laboratory. Our data shows that the common vole invests more energy into gonadal  
416 growth, whereas the tundra vole invests more energy into body mass growth independent of  
417 gonadal growth under LP. This suggests that both body mass growth and gonadal development  
418 are plastic and can be differentially affected by photoperiod, perhaps through different  
419 mechanisms. In Siberian hamsters, the growth hormone (GH) axis is involved in photoperiodic  
420 regulation of body mass (Dumbell et al., 2015; Scherbarth et al., 2015). Our results indicate a  
421 different role for the GH-axis in seasonal body mass regulation in tundra voles and common  
422 voles.

423

#### 424 *Photoperiod induced changes in hypothalamic gene expression*

425 Common vole males show a clear photoperiodic response in both hypothalamic gene  
426 expression and gonadal activation. Genes in the female PNES are strongly regulated by  
427 photoperiod, which is not reflected in gonadal growth. In tundra voles, PNES gene expression  
428 profiles change accordingly to photoperiod, however the gonadal response is less sensitive to  
429 photoperiod, which is similar to the photoperiodic response observed in house mice (Masumoto  
430 et al., 2010). Because the tundra vole is more common at high latitudes, where they live in  
431 tunnels covered by snow in winter and early spring, photoperiodic information might be  
432 blocked during a large part of the year for these animals (Evernden and Fuller, 1972; Korslund,



433 2006). For this reason, other environmental cues, such as metabolic status, may integrate in the  
434 PNES in order to regulate the gonadal response and therefore timing of reproduction.

435

#### 436 *Photoperiod induced changes in $Tsh\beta$ sensitivity*

437 In both vole species  $Tsh\beta$  expression is higher under LP conditions during all stages of  
438 development (Fig. 4C,D), which is in agreement with previous studies in other mammals, birds  
439 and fish (for review see Dardente et al., 2014; Nakane and Yoshimura, 2019). We sampled 17  
440 hours after lights off, when  $Tsh\beta$  expression is peaking. EYA3 is a transcription factor that  
441 binds to the  $Tsh\beta$  promoter, which promotes transcription. Perhaps we sampled too late in  
442 order to find photoperiodic induced changes in  $Eya3$  expression, (Fig. S1A,B), since in mice  
443  $Eya3$  is peaking 12 hours after lights off under LP conditions (Masumoto et al., 2010).

444 TSH binds to its receptor in the tanycytes around the third ventricle. Although, less  
445 pronounced in common voles, elevated  $Tshr$  expression under SP (Fig. 4E,F) may be caused  
446 by low  $Tsh\beta$  levels in the same animals (Fig. 4C,D). In a previous study, a similar relationship  
447 between  $Tshr$  and  $Tsh\beta$  expression in the pars tuberalis and medial basal hypothalamus (MBH)  
448 of Siberian hamsters has been observed (Sáenz de Miera et al., 2017). In our study, the  
449 ependymal paraventricular zone (PVZ) around the third ventricle of the brain and the pars  
450 tuberalis are both included in samples for RNA extraction and qPCR, therefore, we cannot  
451 distinguish between these two brain areas. Brains were collected 17 hours after lights off, when  
452  $Tshr$  mRNA levels in the pars tuberalis and PVZ are predicted to be similar based on studies  
453 in sheep (Hanon et al., 2008). Similar circadian expression patterns are expected in brains of  
454 seasonal long-day breeding rodents. Therefore, the observed increase in  $Tshr$  expression in SP  
455 voles, of both species and sexes, (Fig. 4E,F) may relate to high TSH density in the tanycytes  
456 lining the third ventricle, which might lead to increased TSH sensitivity later in life. The high  
457  $Tshr$  expression in voles developing under SP (Fig. 4E,F) may favour a heightened sensitivity  
458 to increasing TSH, photoperiods increase later in life. This in turn would promote increased  
459 DIO2 and decreased DIO3 levels in spring. Interestingly, photoperiodic responses on  $Tshr$  are  
460 more pronounced in tundra voles than in common voles, suggesting that tundra voles are more  
461 sensitive to TSH protein when raised under SP. However, TSH is a dimer of  $\alpha$ GSU and TSH $\beta$ ,  
462 and we did not measure  $\alpha$ GSU levels in this study.

463 Our vole lab populations are originally from the same latitude in the Netherlands (53°N)  
464 where both populations overlap. This is for the common vole the center (mid-latitude) of its  
465 distribution range, while our lab tundra voles are from a relict population at the lower boundary

466 of its geographical range, which is an extension for this species to operate at southern limits.  
467 For this reason, local adaptation of the PNES may have evolved differently in the two species.  
468 The elevated *Tshr* expression and therefore the possible higher sensitivity to photoperiod in  
469 tundra voles raised under SP, might favour photoperiodic induction of reproduction earlier in  
470 the spring. This might be a strategy to cope with the extremely early spring onset at the low  
471 latitude for this relict tundra vole population.

472 Interestingly, the large peak in *Tsh $\beta$*  expression (Fig. 4C) that is only observed in 21-  
473 day old LP common vole males may be responsible for the drastic increase in testis weight  
474 when animals are 30 days old. Faster testis growth in LP common vole males (Fig. 3C) might  
475 be induced by the 2-3 fold higher *Tsh $\beta$*  levels compared to LP tundra vole males (Fig. 4C).  
476 However, this data have to be interpreted with caution since the current study only considered  
477 gene expression levels and did not investigate protein levels.

478 The reduced *Tshr* expression under LP early in life (Fig. 4E,F) may be induced by  
479 epigenetic mechanisms, such as increased levels of DNA methylation in the promoter of this  
480 gene, which will reduce its transcription. A role for epigenetic regulation of seasonal  
481 reproduction has been proposed based on studies of the adult hamster hypothalamus (Stevenson  
482 and Prendergast, 2013). In order to study the effects of photoperiodic programming in  
483 development, DNA methylation patterns of specific promoter regions of photoperiodic genes  
484 at different circadian time points need to be studied in animals exposed to different  
485 environmental conditions earlier in development.

486

#### 487 *Photoperiod induced changes in hypothalamic Dio2/Dio3 expression*

488 The photoperiodic induced *Tsh $\beta$*  and *Tshr* expression patterns are only reflected in the  
489 downstream *Dio2/Dio3* expression differences in the beginning of development (Fig. 4K,L),  
490 suggesting that this part of the pathway is sensitive to TSH at a very young age. However, *Dio2*  
491 and *Dio3* are also responsive to metabolic status, which can change as a consequence of  
492 changing DIO2/DIO3 levels. Tundra and common vole females show similar photoperiodic  
493 induced *Tsh $\beta$*  patterns, while photoperiodic responses on *Tshr* are larger in tundra voles. The  
494 higher *Tshr* levels in tundra voles may be responsible for the higher *Dio2*, and lower *Dio3*  
495 levels in tundra vole females compared to common vole females. However, the photoperiodic  
496 induced differences in gene expression levels between species is not reflected in female  
497 gonadal weight, indicating that additional signaling pathways are involved in regulating ovary

498 and uterus growth. In males, *Dio2/Dio3* patterns are mainly determined by photoperiod, while  
499 different photoperiodic responses between species are lacking.

500 *Dio2* and *Tsh $\beta$*  expression correlate only at the beginning of development (i.e. 15 and  
501 21 days old) (Fig. 5A-D). These results are partly in agreement with the effects of constant  
502 photoperiod on hypothalamic gene expression in the Siberian hamster, showing induction of  
503 *Dio2* at birth when gestated under LP, and induction of *Dio3* at 15 days old when exposed to  
504 SP (Sáenz de Miera et al., 2017). Furthermore, it is thought that *Dio2/Dio3* expression profiles  
505 will shift due to both photoperiodic and metabolic changes rather than by constant conditions.  
506 Also, negative feedback on the *Dio2/Dio3* system might be induced by changes in metabolic  
507 status. In wild populations of Brandt's voles (*Lasiopodomys brandtii*), seasonal regulation of  
508 these genes, show elevated *Dio2/Dio3* ratios in spring under natural photoperiods, suggesting  
509 the crucial role for those genes in determining the onset of the breeding season in wild  
510 populations (Wang et al., 2019).

511

#### 512 *Photoperiod induced changes in hypothalamic Kiss1 and Npvf expression*

513 In females, both *Kiss1* and *Npvf* expression is higher under LP dependent on age (Fig. S1D,F),  
514 whereas in males no effects of photoperiod on these genes are found (Fig. S1C,E). Other studies  
515 report inconsistent photoperiodic/seasonal effects on ARC *Kiss1* expression in different  
516 species, which may be related to a negative sex steroid feedback on *Kiss1* expressing neurons  
517 (for review see, Simonneaux, 2020). For this reason, sex and species dependent levels of steroid  
518 negative feedback on both *Kiss1* and *Rfrp* expressing neurons in the caudal hypothalamus are  
519 expected.

520

521 In conclusion, our data show that somatic growth is photoperiodic sensitive in the tundra vole  
522 while gonadal growth is photoperiodic sensitive in the common vole. Our finding that the SP  
523 induced *Tshr* expression is more pronounced in the developing hypothalamus of the tundra  
524 vole, may lead to the expectation that programming of TSH sensitivity is an important  
525 regulator of the PNES in this species. Reproductive development seems to be more  
526 dominated by photoperiodic responses in the common vole than in the tundra vole. It is not  
527 excluded that the PNES of the tundra vole has lost its photoperiodic capacity and instead  
528 adopted responses to other environmental variables in its post-glacial relict population at the  
529 southern edge of its distribution. This opens the possibility that the tundra vole has a stronger  
530 response to other environmental cues (e.g. temperature, food, snow cover). Both vole species

531 develop their PNES differently, depending on photoperiod early in development, indicating  
532 that they use environmental cues differently to time reproduction.

533

534 Acknowledgements

535 We would like to thank Saskia Helder for her valuable help in animal care.

536

537 Competing interests

538 No competing interests declared

539

540 Funding

541 This work was funded by the Adaptive Life program of the University of Groningen (B050216  
542 to LvR and RAH), and by the Arctic University of Norway (to JvD and DGH).

543 References

- 544 **Baker, J.** (1938). The evolution of breeding seasons. *Evol. Essays Asp. Evol. Biol.* 161–177.
- 545 **Caro, S. P., Schaper, S. V., Hut, R. A., Ball, G. F. and Visser, M. E.** (2013). The Case of  
546 the Missing Mechanism: How Does Temperature Influence Seasonal Timing in  
547 Endotherms? *PLoS Biol.* **11**,.
- 548 **Dalum, J. Van, Melum, V. J., Wood, S. H. and Hazlerigg, D. G.** (2020). Maternal  
549 photoperiodic programming: melatonin and seasonal synchronization before birth.  
550 *Front. Endocrinol. (Lausanne).* **10**, 1–7.
- 551 **Dardente, H., Wyse, C. A., Birnie, M. J., Dupré, S. M., Loudon, A. S. I., Lincoln, G. A.**  
552 **and Hazlerigg, D. G.** (2010). A molecular switch for photoperiod responsiveness in  
553 mammals. *Curr. Biol.* **20**, 2193–2198.
- 554 **Dardente, H., Hazlerigg, D. G. and Ebling, F. J. P.** (2014). Thyroid hormone and seasonal  
555 rhythmicity. *Front. Endocrinol. (Lausanne).* **5**, 1–11.
- 556 **Dardente, H., Wood, S., Ebling, F. and Sáenz de Miera, C.** (2018). An integrative view of  
557 mammalian seasonal neuroendocrinology. *J. Neuroendocrinol.* **31**,.
- 558 **Dumbell, R. A., Scherbarth, F., Diedrich, V., Schmid, H. A., Steinlechner, S. and**  
559 **Barrett, P.** (2015). Somatostatin Agonist Pasireotide Promotes a Physiological State  
560 Resembling Short-Day Acclimation in the Photoperiodic Male Siberian Hamster  
561 (*Phodopus sungorus*). *J. Neuroendocrinol.* **27**, 588–599.
- 562 **Ebling, F. J. P.** (1994). Photoperiodic differences during development in the dwarf hamsters  
563 *phodopus sungorus* and *phodopus campbelli*. *Gen. Comp. Endocrinol.* **95**, 475–482.
- 564 **Evernden, L. N. and Fuller, W. A.** (1972). Light alteration caused by snow and its  
565 importance to subnivean rodents. *J. Zool.* **50**, 1023–1032.
- 566 **Gall, C. Von, Stehle, J. H. and Weaver, D. R.** (2002). Mammalian melatonin receptors:  
567 molecular biology and signal transduction. *Cell Tissue Res* **309**, 151–162.
- 568 **Gall, C. V. O. N., Weaver, D. R., Moek, J., Jilg, A., Stehle, J. H. and Korf, H.-W.** (2005).  
569 Melatonin Plays a Crucial Role in the Regulation of Rhythmic Clock Gene Expression  
570 in the Mouse Pars Tuberalis. *ann. N.Y. Acad. Sci.* **511**, 508–511.
- 571 **Gerkema, M. P., Daan, S., Wilbrink, M., Hop, M. W. and Van Der Leest, F.** (1993).  
572 Phase control of ultradian feeding rhythms in the common vole (*Microtus arvalis*): The  
573 roles of light and the circadian system. *J. Biol. Rhythms* **8**, 151–171.
- 574 **Guerra, M., Blázquez, J. L., Peruzzo, B., Peláez, B., Rodríguez, S., Toranzo, D., Pastor,**  
575 **F. and Rodríguez, E. M.** (2010). Cell organization of the rat pars tuberalis. Evidence  
576 for open communication between pars tuberalis cells, cerebrospinal fluid and tanycytes.

577 *Cell Tissue Res.* **339**, 359–381.

578 **Hanon, E. A., Lincoln, G. A., Fustin, J.-M., Dardente, H., Masson-Pévet, M., Morgan, P.**  
579 **J. and Hazlerigg, D. G.** (2008). Ancestral TSH mechanism signals summer in a  
580 photoperiodic mammal. *Curr. Biol.* **18**, 1147–1152.

581 **Hoffmann, K.** (1973). Effects of short photoperiods on puberty, growth and moult in the  
582 Djungarian hamster (*Phodopus sungorus*). *J. Reprod. Fertil.* **54**, 29–35.

583 **Horton, T. H.** (1984a). Growth and reproductive development of male *Microtus montanus* is  
584 affected by the prenatal photoperiod. *Biol. Reprod.* **31**, 499–504.

585 **Horton, T. H.** (1984b). Growth and reproductive is affected development by the prenatal of  
586 male *Microtus montanus* photoperiod. *Biol. Reprod.* **504**, 499–504.

587 **Horton, T. H.** (1985). Cross-fostering of Voles Demonstrates In Utero Effect of Photoperiod.  
588 *Biol. Reprod.* **33**, 934–939.

589 **Horton, T. H. and Stetson, M. H.** (1992). Maternal transfer of photoperiodic information in  
590 rodents. *Anim. Reprod. Sci.* **30**, 29–44.

591 **Hut, R. A.** (2011). Photoperiodism : Shall EYA Compare Thee to a Summer ' s Day ? *Curr.*  
592 *Biol.* **21**, R22–R25.

593 **Hut, R. A., Paolucci, S., Dor, R., Kyriacou, C. P. and Daan, S.** (2013). Latitudinal clines:  
594 an evolutionary view on biological rhythms. *Proc. R. Soc. B Biol. Sci.* **280**, 20130433–  
595 20130433.

596 **Klosen, P., Hicks, D., Pevet, P. and Felder-Schmittbuhl, M. P.** (2019). MT1 and MT2  
597 melatonin receptors are expressed in nonoverlapping neuronal populations. *J. Pineal*  
598 *Res.* **67**, 1–19.

599 **Korslund, L.** (2006). Activity of root voles (*Microtus oeconomus*) under snow: Social  
600 encounters synchronize individual activity rhythms. *Behav. Ecol. Sociobiol.* **61**, 255–  
601 263.

602 **Król, E., Douglas, A., Dardente, H., Birnie, M. J., Vinne, V. van der, Eijer, W. G.,**  
603 **Gerkema, M. P., Hazlerigg, D. G. and Hut, R. A.** (2012). Strong pituitary and  
604 hypothalamic responses to photoperiod but not to 6-methoxy-2-benzoxazolinone in  
605 female common voles (*Microtus arvalis*). *Gen. Comp. Endocrinol.* **179**, 289–295.

606 **Lechan, R. M. and Fekete, C.** (2005). Role of thyroid hormone deiodination in the  
607 hypothalamus. *Thyroid* **15**, 883–897.

608 **Magner, J. A.** (1990). Thyroid-Stimulating Hormone: Biosynthesis, Cell Biology, and  
609 Bioactivity. **11**, 354–385.

610 **Malyshev, A. V, Henry, H. A. L. and Kreyling, J.** (2014). Relative effects of temperature

611 vs photoperiod on growth and cold acclimation of northern and southern ecotypes of the  
612 grass *Arrhenatherum elatius*. *Environ. Exp. Bot.* **106**, 189–196.

613 **Masumoto, K. H., Ukai-Tadenuma, M., Kasukawa, T., Nagano, M., Uno, K. D., Tsujino,**  
614 **K., Horikawa, K., Shigeyoshi, Y. and Ueda, H. R.** (2010). Acute induction of *Eya3* by  
615 late-night light stimulation triggers TSH $\beta$  expression in photoperiodism. *Curr. Biol.* **20**,  
616 2199–2206.

617 **Nakane, Y. and Yoshimura, T.** (2019). Photoperiodic Regulation of Reproduction in  
618 Vertebrates. *Annu. Rev. Anim. Biosci.* **7**, 173–94.

619 **Nakao, N., Ono, H., Yamamura, T., Anraku, T., Takagi, T., Higashi, K., Yasuo, S.,**  
620 **Katou, Y., Kageyama, S., Uno, Y., et al.** (2008). Thyrotrophin in the pars tuberalis  
621 triggers photoperiodic response. *Nature* **452**, 317–322.

622 **Ono, H., Hoshino, Y., Yasuo, S., Watanabe, M., Nakane, Y., Murai, A., Ebihara, S.,**  
623 **Korf, H.-W. and Yoshimura, T.** (2008). Involvement of thyrotropin in photoperiodic  
624 signal transduction in mice. *Proc. Natl. Acad. Sci.* **105**, 18238–18242.

625 **Peacock, J. M.** (1976). Temperature and leaf growth in four grass species. *J. Appl. Ecol.* **13**,  
626 225–232.

627 **Pfaffl, M. W.** (2001). A new mathematical model for relative quantification in real-time RT-  
628 PCR. *Nucleic Acids Res.* **29**, 16–21.

629 **Phalen, A. N., Wexler, R., Cruickshank, J., Park, S. and Place, N. J.** (2009). Photoperiod-  
630 induced differences in uterine growth in *Phodopus sungorus* are evident at an early age  
631 when serum estradiol and uterine estrogen receptor levels are not different. *Comp.*  
632 *Biochem. Physiol. - A Mol. Integr. Physiol.* **155**, 115–121.

633 **Prendergast, B. J., Gorman, M. R. and Zucker, I.** (2000). Establishment and persistence of  
634 photoperiodic memory in hamsters. *Proc. Natl. Acad. Sci. U. S. A.* **97**, 5586–5591.

635 **Prendergast, B. J., Pyter, L. M., Kampf-Lassin, A., Patel, P. N. and Stevenson, T. J.**  
636 (2013). Rapid induction of hypothalamic iodothyronine deiodinase expression by  
637 photoperiod and melatonin in juvenile Siberian hamsters (*Phodopus sungorus*).  
638 *Endocrinology* **154**, 831–841.

639 **Robson, M. J.** (1967). A comparison of british and North African varieties of tall fescue  
640 (*Festuca arundinacea*). I. Leaf growth during winter and the effects on it of temperature  
641 and daylength. *J. Appl. Ecol.* **4**, 475–484.

642 **Sáenz de Miera, C., Bothorel, B., Jaeger, C., Simonneaux, V. and Hazlerigg, D.** (2017).  
643 Maternal photoperiod programs hypothalamic thyroid status via the fetal pituitary gland.  
644 *Proc. Natl. Acad. Sci.* **114**, 8408–8413.

645 **Sáenz de Miera, C., Beymer, M., Routledge, K., Król, E., Selman, C., Hazlerigg, D. G.**  
646 **and Simonneaux, V.** (2020). Photoperiodic regulation in a wild-derived mouse strain. *J.*  
647 *Exp. Biol.* **223**, 1–9.

648 **Sáenz De Miera, C.** (2019). Maternal photoperiodic programming enlightens the internal  
649 regulation of thyroid-hormone deiodinases in tanycytes. *J. Neuroendocrinol.* **31**, 12679.

650 **Sáenz De Miera, C., Monecke, S., Bartzen-Sprauer, J., Laran-Chich, M. P., Pévet, P.,**  
651 **Hazlerigg, D. G. and Simonneaux, V.** (2014). A circannual clock drives expression of  
652 genes central for seasonal reproduction. *Curr. Biol.* **24**, 1500–1506.

653 **Scherbarth, F., Diedrich, V., Dumbell, R. A., Schmid, H. A., Steinlechner, S. and**  
654 **Barrett, P.** (2015). Somatostatin receptor activation is involved in the control of daily  
655 torpor in a seasonal mammal. *Am J Physiol Regul Integr Comp Physiol* **309**, 668–674.

656 **Simonneaux, V.** (2020). A Kiss to drive rhythms in reproduction. *Eur. J. Neurosci.* **51**, 509–  
657 530.

658 **Stetson, M. H., Elliott, J. A. and Goldman, B. D.** (1986). Maternal transfer of  
659 photoperiodic information influences the photoperiodic response of prepubertal  
660 Djungarian hamsters (*Phodopus sungorus sungorus*). *Biol. Reprod.* **34**, 664–669.

661 **Stevenson, T. J. and Prendergast, B. J.** (2013). Reversible DNA methylation regulates  
662 seasonal photoperiodic time measurement. *Proc. Natl. Acad. Sci.* **110**, 4644–4646.

663 **Stumpfel, S., Bieber, C., Blanc, S., Ruf, T. and Giroud, S.** (2017). Differences in growth  
664 rates and pre-hibernation body mass gain between early and late-born juvenile garden  
665 dormice. *J. Comp. Physiol. B* **187**, 253–263.

666 **Team, R. C.** (2013). R: A language and environment for statistical computing. *R Found. Stat.*  
667 *Comput. Vienna, Austria.*

668 **Tkadlec, E.** (2000). The effects of seasonality on variation in the length of breeding season  
669 in arvicoline rodents. *Folia Zool.* **49**, 269–286.

670 **van de Zande, L., van Apeldoorn, R. C., Blijdenstein, A. F., de Jong, D., van Delden, W.**  
671 **and Bijlsma, R.** (2000). Microsatellite analysis of population structure and genetic  
672 differentiation within and between populations of the root vole, *Microtus oeconomus* in  
673 the Netherlands. *Mol. Ecol.* **9**, 1651–1656.

674 **Wang, D., Li, N., Tian, L., Ren, F., Li, Z., Chen, Y., Liu, L., Hu, X., Zhang, X., Song, Y.,**  
675 **et al.** (2019). Dynamic expressions of hypothalamic genes regulate seasonal breeding in  
676 a natural rodent population. *Mol. Ecol.* **28**, 3508–3522.

677 **Wickham, H.** (2016). *ggplot2: Elegant Graphics for Data Analysis*. Springer-Verlag New  
678 York.



679 **Williams, L. M. and Morgan, P. J.** (1988). Demonstration of melatonin-binding sites on the  
680 pars tuberalis of the rat. *J. Endocrinol.* **119**, 1–3.

681 **Wood, S. H., Christian, H. C., Miedzinska, K., Saer, B. R. C., Johnson, M., Paton, B.,**  
682 **Yu, L., McNeilly, J., Davis, J. R. E., McNeilly, A. S., et al.** (2015). Binary switching  
683 of calendar cells in the pituitary defines the phase of the circannual cycle in mammals.  
684 *Curr. Biol.* **25**, 2651–2662.

685 **Yellon, S. M. and Goldman, B. D.** (1984). Photoperiod Control of Reproductive  
686 Development in the Male Djungarian Hamster ( *Phodopus sungorus* )\*. *Endocrinology*  
687 **114**, 664–670.

688

689

690 Supplementary information

691 **Table S1**

692 *Preparation 40 µL Reversed-Transcription reactions concentrations of components used for RT*

Component	Stock concentration	Final concentration
Oligo(dT) <sub>18</sub>	100 µM	5 µM
5X Reaction buffer	5X	1X
RiboLock RNase Inhibitor	20 U/µL	1 U/µL
dNTP Mix	10 mM	1 mM
RevertAid H Minus Reverse Transcriptase	200 U/µL	10 U/µL
Template RNA	0.1 µg/µl	1 µg/µl

693

694

695 **Table S2**

696 *Primers used for qPCR. Primer sequences were gene specific for M. arvalis and M. oeconomus, except for Tshβ*  
697 *reversed and Tshr forward for M. arvalis, and Dio3 forward and Eya3 reversed for M. oeconomus, which differ*  
698 *in 1 nucleotide from the used primers.*

Gene	Forward primer sequence (‘5-‘3)	Reverse primer sequence (‘5-‘3)
<i>Dio2</i>	CAGCCAACCTCCGGACTTCTT	GCCGACTTCCTGTTGGTGTA
<i>Dio3</i>	CAAGCATTTTCTGCGTCGTC	GATACGCAGATGGGTGGGTC
<i>Dnmt1</i>	TAGCCACCAAACGAAGACCC	GTTCGAGCCGCCTTTTTTCTC
<i>Dnmt3a</i>	GAGAGGGAACGAGACCCCA	CCCGTTTCCGTTTGCTGATG
<i>Eya3</i>	TGTTGGGTTTCACTCCCTG	GGCAAAGTAAGCAGGTGTA

<i>Gapdh</i>	GCTGCCCAGAACATCATCCCTG	GACGACGGACACATTGGGGGTA
<i>Kiss1</i>	CCATGCCACCGGTTGAGAG	GCCGAAGGAGTTCCAGTTGT
<i>Mtnr1a</i>	ATCGCCATTAACCGCTACTG	GAGAGTTCCGGTTTGCAGGT
<i>Npvf</i>	AGGCAGGGATCTTGAACCAC	TCTCTGTAGCCAGCGACTCA
<i>Tsh<math>\beta</math></i>	GCTTATGGCAACAGGGTAGGA	AATACGCGCTCTCCCAGGAT
<i>Tshr</i>	ATCCCCAGTCTCGCGTTTTTC	GCTTCTGGTGTTGCGGATTT

699

700

701 **Table S3**

702 *Thermal cycling conditions for qPCR.*

qPCR step	T (°C)	Duration (seconds)	Cycles	
Enzyme activation	95	180	Hold	704
Denaturation	95	3	40	705
Annealing/ extension/ data acquisition	60	20	40	706 707 708
Dissociation	95	3		709
	65	5		710
	95	15		711
				712

713

714

715

716

717

718

719

720

721

722

723

724

725

726

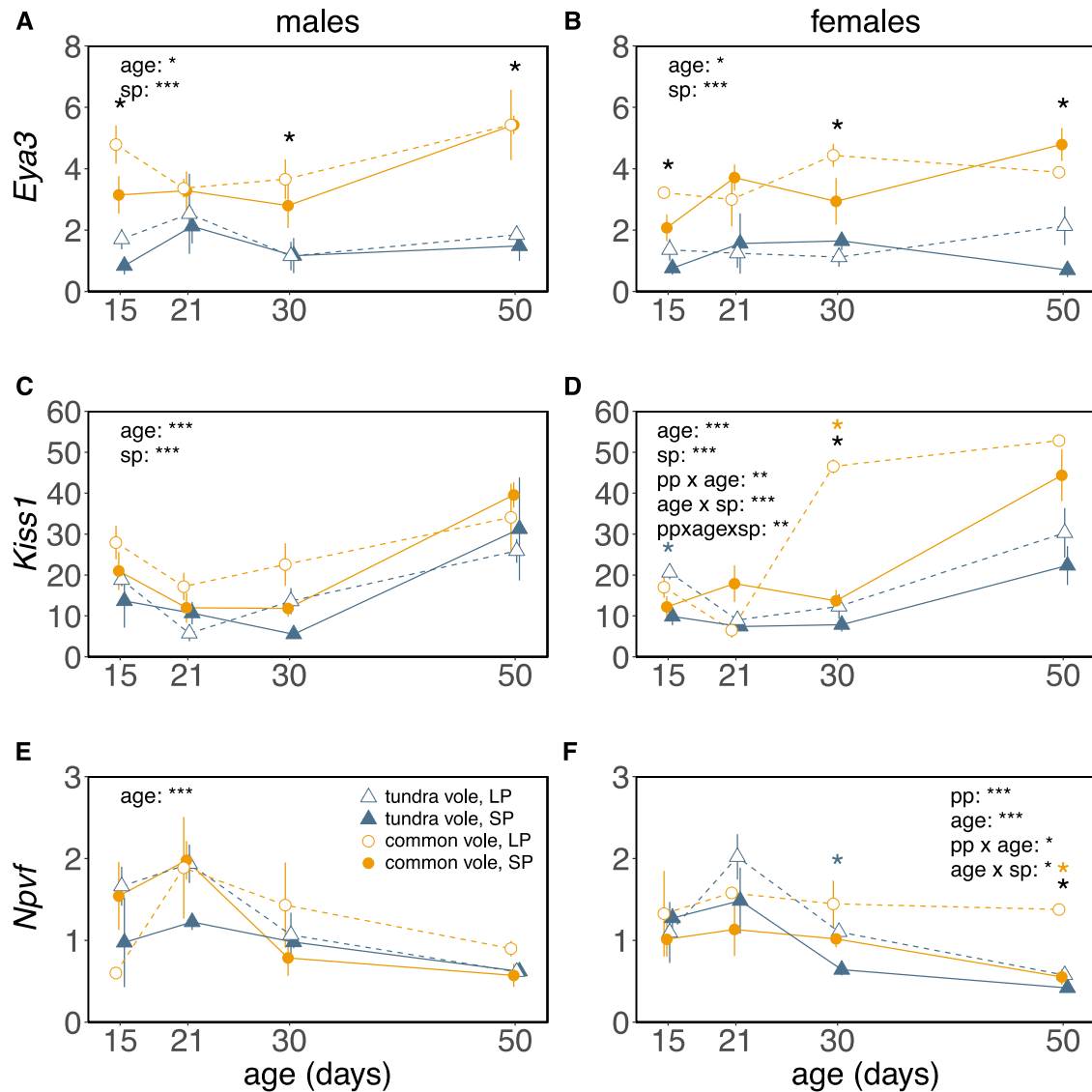
727

	body mass (m)				gonads (m)				GSI (m)			
	Df	SS	F	p	Df	SS	F	p	Df	SS	F	p
pp	1,66		22.5261	< 0.001	1,56	0.4619	118.426	< 0.001	1,56	7.172	132.347	< 0.001
age	1,76		320.7922	< 0.001	3,56	0.9478	80.998	< 0.001	3,56	8.307	51.101	< 0.001
species	1,66		58.5611	< 0.001	1,56	0.0337	8.641	< 0.01	1,56	0.247	4.551	< 0.05
pp:age	1,76		6.8905	< 0.001	3,56	0.1169	9.994	< 0.001	3,56	1.042	6.411	< 0.001
pp:species	1,66		7.9873	< 0.05	1,56	0.0011	0.276	ns	1,56	1.033	19.060	< 0.001
age:species	1,76		44.6027	< 0.001	3,56	0.0352	3.012	< 0.05	3,56	0.028	0.171	ns
pp:age:species	1,76		0.0826	ns	3,56	0.0028	0.238	ns	3,56	0.354	2.175	ns
<i>Mtnr1a</i> (m)					<i>Tshb</i> (m)					<i>Tshr</i> (m)		
	Df	SS	F	p	Df	SS	F	p	Df	SS	F	p
pp	1,42	0.12	0.080	ns	1,42	65.07	78.822	< 0.001	1,42	4.303	33.364	< 0.001
age	3,42	4.23	0.936	ns	3,42	11.45	4.625	< 0.01	3,42	1.613	4.170	< 0.05
species	1,42	4.37	2.899	ns	1,42	4.15	5.028	< 0.05	1,42	9.763	75.709	< 0.001
pp:age	3,42	0.85	0.188	ns	3,42	9.18	3.708	< 0.05	3,42	0.690	1.783	ns
pp:species	1,42	2.53	1.676	ns	1,42	2.55	3.084	ns	1,42	1.053	8.165	< 0.01
age:species	3,42	1.17	0.258	ns	3,42	7.26	2.933	< 0.05	3,42	0.320	0.827	ns
pp:age:species	3,42	6.03	1.333	ns	3,42	8.91	3.596	< 0.05	3,42	0.953	2.464	ns
<i>Dio2</i> (m)					<i>Dio3</i> (m)					<i>Dio2/Dio3</i> (m)		
	Df	SS	F	p	Df	SS	F	p	Df	SS	F	p
pp	1,42	1.409	14.702	< 0.001	1,42	41.7	4.838	< 0.05	1,42	10.25	8.537	< 0.01
age	3,42	0.771	2.683	ns	3,42	74.6	2.885	< 0.05	3,42	7.18	1.994	ns
species	1,42	0.018	0.188	ns	1,42	7.6	0.878	ns	1,42	0.32	0.267	ns
pp:age	3,42	0.418	1.456	ns	3,42	3.3	0.129	ns	3,42	2.74	0.760	ns
pp:species	1,42	0.002	0.017	ns	1,42	10.1	1.173	ns	1,42	0.01	0.008	ns
age:species	3,42	0.540	1.877	ns	3,42	14.1	0.545	ns	3,42	5.82	1.617	ns
pp:age:species	3,42	4.025	0.897	ns	3,42	6.0	0.233	ns	3,42	3.94	1.095	ns
<i>Eya3</i> (m)					<i>Kiss1</i> (m)					<i>Npvf</i> (m)		
	Df	SS	F	p	Df	SS	F	p	Df	SS	F	p
pp	1,42	3.47	1.722	ns	1,42	237	2.956	ns	1,42	0.253	0.606	ns
age	3,42	22.49	3.716	< 0.05	3,42	5092	21.186	< 0.001	3,42	12.769	10.205	< 0.001
species	1,42	96.66	47.928	< 0.001	1,42	1252	15.621	< 0.001	1,42	0.280	0.672	ns
pp:age	3,42	2.22	0.367	ns	3,42	240	0.998	ns	3,42	0.572	0.457	ns
pp:species	1,42	3.73	1.850	ns	1,42	186	2.325	ns	1,42	0.056	0.134	ns
age:species	3,42	12.50	2.066	ns	3,42	172	0.715	ns	3,42	1.061	0.848	ns
pp:age:species	3,42	0.15	0.025	ns	3,42	80	0.331	ns	3,42	2.373	1.896	ns
<i>Dnmt1</i> (m)					<i>Dnmt3a</i> (m)							
	Df	SS	F	p	Df	SS	F	p				
pp	1,42	1.19	0.676	ns	1,42	1.41	0.767	ns				
age	3,42	76.07	14.377	< 0.001	3,42	3.58	0.651	ns				
species	1,42	7.79	4.419	< 0.05	1,42	11.78	6.413	< 0.05				
pp:age	3,42	4.21	0.796	ns	3,42	1.93	0.350	ns				
pp:species	1,42	3.33	1.886	ns	1,42	0.04	0.023	ns				
age:species	3,42	4.72	0.892	ns	3,42	3.08	0.558	ns				
pp:age:species	3,42	15.91	3.008	< 0.05	3,42	7.72	1.401	ns				
body mass (f)					gonads (f)					GSI (f)		
	Df	SS	F	p	Df	SS	F	p	Df	SS	F	p
pp	1,60		14.9452	< 0.001	1,50	0.0000919	1.575	ns	1,50	0.00002	0.0111	ns
age	1,78		169.3274	< 0.001	3,50	0.0006542	3.737	< 0.05	3,50	0.04933	8.281	< 0.001
species	1,60		17.4063	< 0.001	1,50	0.0004270	7.316	< 0.01	1,50	0.05081	25.592	< 0.001
pp:age	1,78		0.0398	ns	3,50	0.0003350	1.913	ns	3,50	0.00869	1.459	ns
pp:species	1,60		9.0244	< 0.01	1,50	0.0004222	7.235	< 0.01	1,50	0.00805	4.052	< 0.05
age:species	1,78		13.0245	< 0.001	3,50	0.0005309	3.033	< 0.05	3,50	0.01784	2.995	< 0.05
pp:age:species	1,78		0.2721	ns	3,50	0.0003238	1.850	ns	3,50	0.01251	2.101	ns
<i>Mtnr1a</i> (f)					<i>Tshβ</i> (f)					<i>Tshr</i> (f)		
	Df	SS	F	p	Df	SS	F	p	Df	SS	F	p
pp	1,40	1.59	1.593	ns	1,40	128.65	127.264	< 0.001	1,40	0.869	4.687	< 0.05
age	3,40	27.14	9.041	< 0.001	3,40	4.92	1.621	ns	3,40	1.213	2.182	ns
species	1,40	0.08	0.084	ns	1,40	0.09	0.088	ns	1,40	12.811	69.096	< 0.001
pp:age	3,40	3.90	1.300	ns	3,40	5.17	1.706	ns	3,40	0.687	1.234	ns
pp:species	1,40	0.06	0.057	ns	1,40	0.02	0.018	ns	1,40	0.193	1.043	ns
age:species	3,40	1.95	0.648	ns	3,40	1.16	0.382	ns	3,40	1.277	2.297	ns
pp:age:species	3,40	0.90	0.299	ns	3,40	2.31	0.761	ns	3,40	0.329	0.592	ns
<i>Dio2</i> (f)					<i>Dio3</i> (f)					<i>Dio2/Dio3</i> (f)		
	Df	SS	F	p	Df	SS	F	p	Df	SS	F	p
pp	1,40	0.422	2.065	ns	1,40	9.07	2.206	ns	1,40	26.29	5.976	< 0.05
age	3,40	3.262	5.318	< 0.01	3,40	81.75	6.629	< 0.001	3,40	34.84	2.640	ns
species	1,40	1.408	6.886	< 0.05	1,40	25.09	6.105	< 0.05	1,40	6.69	1.522	ns
pp:age	3,40	1.088	1.775	ns	3,40	4.39	0.356	ns	3,40	36.77	2.786	ns
pp:species	1,40	0.010	0.047	ns	1,40	14.61	3.555	ns	1,40	6.16	1.399	ns
age:species	3,40	1.674	2.730	ns	3,40	50.15	4.067	< 0.05	3,40	10.51	0.796	ns
pp:age:species	3,40	0.168	0.273	ns	3,40	16.20	1.314	ns	3,40	35.21	2.668	ns
<i>Eya3</i> (f)					<i>Kiss1</i> (f)					<i>Npvf</i> (f)		

	Df	SS	F	p	Df	SS	F	p	Df	SS	F	p
pp	1,40	0.32	0.303	ns	1,40	191	4.057	ns	1,40	3.785	14.783	< 0.001
age	3,40	10.62	3.351	< 0.05	3,40	4491	31.856	< 0.001	3,40	10.547	13.730	< 0.001
species	1,40	60.63	57.392	< 0.001	1,40	1345	28.629	< 0.001	1,40	0.796	3.108	ns
pp:age	3,40	2.99	0.943	ns	3,40	680	4.820	< 0.01	3,40	2.698	3.513	< 0.05
pp:species	1,40	0.02	0.021	ns	1,40	3	0.061	ns	1,40	1.123	4.385	< 0.05
age:species	3,40	5.07	1.601	ns	3,40	978	6.938	< 0.001	3,40	0.458	0.596	ns
pp:age:species	3,40	6.82	2.153	ns	3,40	843	5.980	< 0.01	3,40	0.876	1.140	ns

728 **Table S4.** Statistics for type I two-way ANOVA's

729



730

731 **Figure S1. Effects of constant photoperiod on gene expression levels in the developing hypothalamus.**

732 Relative gene expression levels of (A, B) *Eya3*, (C, D) *Kiss1*, (E, F) *Npvf* expression in the hypothalamus of  
 733 developing common (orange circles) and tundra vole (blue triangles) males and females respectively, under LP  
 734 (open symbols, dashed lines) or SP (closed symbols, solid lines). Lines connect averages representing non-  
 735 repeated measures. Data are mean±s.e.m.. Male tundra vole LP: n=16, male tundra vole SP: n=13, male  
 736 common vole LP n=14, male common vole SP n=15. female tundra vole LP: n=16, female tundra vole SP:  
 737 n=16, female common vole LP n=8, female common vole SP n=16. Significant effects (ANOVA, post-hoc  
 738 Tukey) of photoperiod at specific ages are indicate for tundra voles (blue asterisks) and common voles (orange

739 asterisks), significant effects of species are indicated by black asterisks. Significant effects of: photoperiod (pp),  
740 age (age), species (sp) and interactions are shown in each graph, \*p < 0.05, \*\*p < 0.01, \*\*\*p < 0.001. Statistic  
741 results for two-way ANOVA's (photoperiod, age and species) can be found in table S4.  
742